

A novel large-pore framework titanium silicate catalyst

Paula Brandão,^a Anabela Valente,^a Andreas Philippou,^b Artur Ferreira,^c Michael W. Anderson^b and João Rocha^{*a}

^aDepartment of Chemistry, University of Aveiro, 3810-193 Aveiro, Portugal.

E-mail: rocha@dq.ua.pt

^bDepartment of Chemistry, UMIST, PO Box 88, Manchester, UK M60 1QD

^cESTGA, University of Aveiro, 3810-193 Aveiro, Portugal

Received 29th April 2002, Accepted 2nd October 2002

First published as an Advance Article on the web 15th October 2002

The synthesis and characterisation of AM-18 (Aveiro-Manchester structure number 18), a large-pore framework sodium titanium silicate catalyst, is reported. The as-synthesised material was characterised by powder X-ray diffraction (XRD), thermogravimetry (TGA) and differential thermal analysis (DTA), scanning electron microscopy (SEM) and chemical analysis by energy dispersive analysis of X-rays (EDAX), nitrogen and benzene adsorption measurements, ²³Na triple-quantum (MQ) magic angle-spinning (MAS) and ²⁹Si MAS NMR, Fourier transform infrared (FTIR) and Raman spectroscopies. The latter two techniques indicate that this novel titanium silicate may contain five-coordinated titanium. AM-18 shows high thermostability (in excess of 650 °C). Isopropanol conversion was used as a model reaction to study the acid–base properties of as-synthesised AM-18. This material exhibits high catalytic activity (71% conversion) and selectivity for propene (74%).

Introduction

Since the discovery of TS-1, an excellent catalyst for a wide range of selective oxidation reactions with aqueous H₂O₂ as oxidant,¹ titanium has been incorporated into the framework of several zeolites^{2,3} and mesoporous materials.^{4,7} In all these materials titanium is tetrahedrally-coordinated to oxygen. Later, a new family of microporous silicates possessing framework Ti(IV) in octahedral coordination and known as ETS (Engelhard titanium silicate) materials, has been reported.^{8,9} This early work stimulated research into the synthesis and characterisation of novel mixed octahedral–tetrahedral framework silicates.¹⁰ A much smaller class of titanium silicates are those formed by tetrahedral silicon and five-coordinated titanium. AM-1¹¹ or JDF-L1¹² and ETS-4¹³ are the only synthetic titanium silicates containing titanium in such coordination. AM-1 and JDF-L1, with a composition Na₄Ti₂Si₈O₂₂·4H₂O, is an unusual non-centrosymmetric tetragonal layered solid that contains five-coordinated Ti(IV) ions in the form of TiO₅ square pyramids in which each of the vertices of the base is linked to SiO₄ tetrahedra to form continuous sheets. ETS-4, a microporous material, is essentially the synthetic analogue of the mineral zorite.¹⁴ It contains O–Ti(IV)–O chains, where titanium is coordinated to five or six oxygen atoms.

In recent years we have been interested in the synthesis of open framework metal silicates with potential applications in adsorption, separation, catalysis and ion exchange, particularly vanadium,^{15,16} zirconium,¹⁷ niobium^{18–20} and tin silicates.²¹ We now wish to report on the synthesis and characterisation of a novel large-pore titanium silicate named AM-18 (Aveiro-Manchester structure number 18). Infrared and Raman spectroscopies suggest that AM-18 possesses five-coordinated framework Ti. Accordingly, AM-18 together with AM-1 and ETS-4 are the only three synthetic titanium silicate materials containing Ti in such a coordination. In addition, the presence of some six-coordinated Ti in AM-18 can not be discarded.

Experimental

Synthesis of AM-18

The synthesis of AM-18 was carried out in teflon-lined autoclaves under static hydrothermal conditions. An alkaline

solution was prepared by mixing 5.00 g sodium silicate solution (Merck), 15.22 g H₂O, 1.33 g NaOH (Merck), 5.82 g TiCl₃ solution (10% in HCl, Merck) was added to that solution and stirred thoroughly. This gel with a molar composition of 2.9 Na₂O:4.0 SiO₂:TiO₂:149.7 H₂O, was autoclaved for 2 days at 230 °C without agitation. The solid was filtered, washed with distilled water and dried at room temperature, giving an off-white microcrystalline powder.

Characterisation

Powder XRD data were collected on an X'Pert MPD Philips diffractometer (CuK_α X-radiation) with a curved graphite monochromator, an automatic divergence slit (irradiated length 20.00 mm), a progressive receiving slit (slit's height 0.05 mm) and a flat plate sample holder, in a Bragg–Brentano para-focusing optics configuration. Intensity data were collected by the step counting method (step 0.02°, time 38 s) in the range 2θ 3–32°. X-ray diffraction pattern auto-indexing was performed with the CRYSFIRE System²² from the resolved first 20 lines and checked with the Checkcell package.²³

SEM images were recorded on a Hitachi S-4100 Field Emission Gun tungsten filament working with a voltage of 25000 V. The chemical composition was determined by energy dispersive analysis of X-rays (EDAX). TGA and DTA analyses were carried out in a SDT 2960 simultaneous DTA-TGA thermal analyser 2000 TA instrument. The sample was heated in air with a rate of 10 °C min⁻¹. Nitrogen adsorption measurements at 77 K were performed using a Micromeritics ASAP 2010 V1.01 B automatic instrument. Pore size distributions were determined using the density-functional theory (DFT) Plus Software for data files generated from the ASAP instrument. Adsorption of benzene, *m*-xylene and mesitylene was measured at 298 K, using a gravimetric adsorption apparatus equipped with a CI electronic MK2-M5 microbalance and an Edwards Barocel pressure sensor. Before adsorptions measurements, the sample was outgassed overnight at 573 K. ²⁹Si and ²³Na solid-state NMR spectra were recorded at 79.49 and 105.81 MHz (9.4 T) on a Bruker Avance 400 spectrometer. ²⁹Si magic angle spinning (MAS) NMR spectrum was measured with 40° pulses, a spinning rate of 5.0 kHz, and a recycle delay of 35 s. Chemical shifts are quoted in ppm from

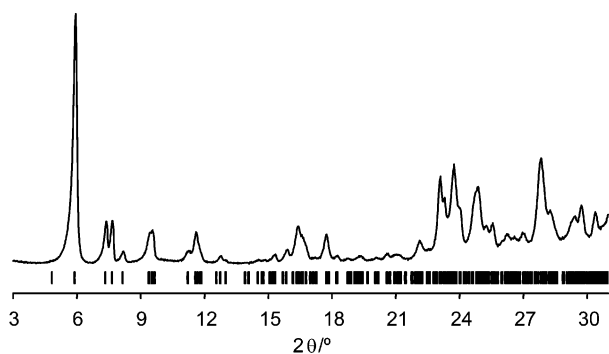


Fig. 1 Experimental powder XRD pattern of AM-18. The tick marks depict Bragg reflections.

TMS. ^{23}Na FAM II MQ MAS NMR spectrum: the length of the first rf pulse was $3.65\ \mu\text{s}$ (magnetic field amplitude $B_1 = 170\ \text{kHz}$), the FAM II block consisted of 4 (X, -X, X, -X) fast amplitude modulated pulses with 1.35, 0.70, 0.55 and $0.40\ \mu\text{s}$ length. The length of the soft pulse (z-filter) was $12.5\ \mu\text{s}$ (magnetic field amplitude $B_1 = 10\ \text{kHz}$). The MAS rate was $\nu_R = 15\ \text{kHz}$. 128 points were acquired in the t_1 dimension in increments of $1/\nu_R = 67\ \mu\text{s}$. The ppm scale of the sheared spectra is referenced to ν_0 frequency in the ν_2 domain and to $3.78\ \nu_0$ in the ν_1 domain (ref. 1 M aqueous NaCl). FTIR spectra were recorded in absorbance mode on a Mattson Mod 7000 FTIR spectrophotometer using KBr pellets in a range $400\text{--}4000\ \text{cm}^{-1}$. The pellets were prepared by sample dispersion (0.2 mg) in a KBr matrix (150 mg) and pressed. The spectra were typically an average of 64 scans with $4\ \text{cm}^{-1}$ resolution. The Raman spectra were recorded with a Bruker RFS100/S FT instrument (Nd: YAG laser, 1064 nm excitation, InGaAs detector).

Catalytic experiments

The isopropanol reaction was carried out at atmospheric pressure in a fixed-bed stainless-steel reactor (height = 16 cm, internal diameter = 0.5 cm), which was charged with 50 mg of catalyst. Prior to reaction, the catalyst was activated at $350\ ^\circ\text{C}$ in a flow of argon ($10\ \text{ml min}^{-1}$). The reactant is fed using a syringe pump and mixed with the flowing gas before entering the reactor tube. The Ar/reactant molar ratio in the feed was 16, corresponding to isopropanol partial pressure of $\approx 6\ \text{kPa}$. The products were analysed by gas chromatography with a 30 meter long capillary column (DP1 fused silica phase) and a FID (flame ionisation detector).

Results and discussion

The powder XRD pattern of titanium silicate AM-18 and correspondent d -spacing and intensities are shown in Fig. 1 and Table 1, respectively. The AM-18 cell is monoclinic with $a = 23.565(3)$, $b = 30.018(3)$, $c = 12.282(2)\ \text{\AA}$, $\beta = 101.00(1)$ ($V = 8528\ \text{\AA}^3$). The most probable space group is $C2/m$.

SEM images (Fig. 2) reveal that AM-18 crystals consist of thin plates with an average lateral particle size of *ca.* $5\ \mu\text{m}$. A small amount of amorphous material is present in the samples studied. EDAX chemical analysis gives Si/Ti and Na/Ti molar ratios of 3.3 and 1.5, respectively.

Powder XRD patterns recorded *in situ* show that AM-18 is stable up to temperatures in excess of $650\ ^\circ\text{C}$. The AM-18 total mass loss between 30 and $700\ ^\circ\text{C}$ is *ca.* 15.5%. The DTA curve (Fig. 3) exhibits an endothermic peak centred at *ca.* $120\ ^\circ\text{C}$, assigned to the loss of physisorbed water, and an exothermic peak centred at *ca.* $675\ ^\circ\text{C}$, which may be associated with structure collapse.

Nitrogen adsorption isotherm is of type I with a slightly

Table 1 Powder XRD data of AM-18

$d/\text{\AA}$	I/I_0	$d/\text{\AA}$	I/I_0
14.875	100	4.581	6
11.969	19	4.422	5
11.550	19	4.312	7
10.805	7	4.199	6
9.374	15	4.016	12
9.278	16	3.941	9
7.851	8	3.853	37
7.622	15	3.821	28
6.920	6	3.745	42
6.808	4	3.709	25
6.090	4	3.593	31
5.982	4	3.577	33
5.770	6	3.523	17
5.568	8	3.483	18
5.410	17	3.425	12
5.342	14	3.397	14
5.146	5	3.351	13
4.999	15	3.304	15
4.856	6	3.208	43
4.743	5	3.155	24

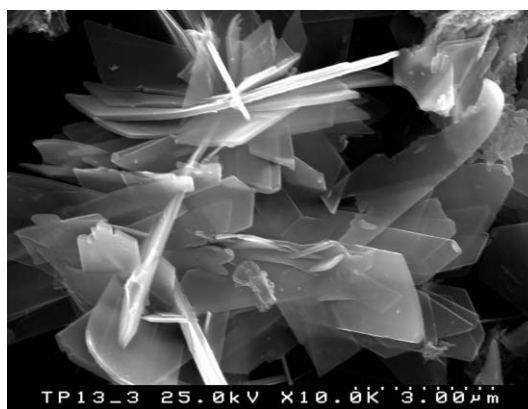


Fig. 2 SEM image of AM-18 crystals.

upward distortion, suggesting that microporosity is associated with significant external surface (Fig. 4). The Langmuir specific surface area is *ca.* $451\ \text{m}^2\ \text{g}^{-1}$ and the micropore volume estimated from the t-plot (using the Harkins-Jura equation, $R^2 = 0.998$) is $0.14\ \text{cm}^3\ \text{g}^{-1}$ (Fig. 5). The median pore width is estimated to be $6.8\ \text{\AA}$ by the DFT method. Adsorption of benzene (kinetic diameter of $5.85\ \text{\AA}$) at 298 K also reflects the occurrence of micropore filling phenomenon and gives a Langmuir area of $419\ \text{m}^2\ \text{g}^{-1}$ (taking $42.3\ \text{\AA}^2$ as the average area occupied by a C_6H_6 molecule lying flat in the monolayer)

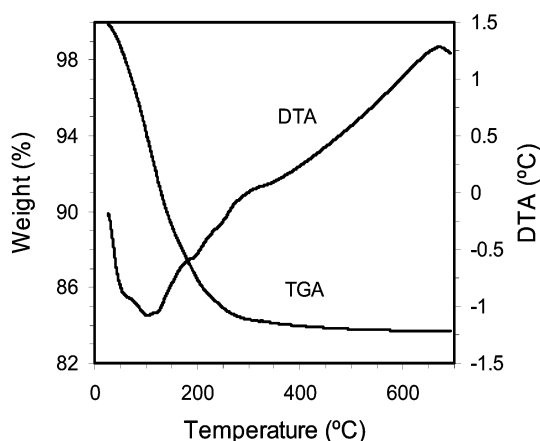


Fig. 3 TGA and DTA curves, recorded in air, of AM-18.

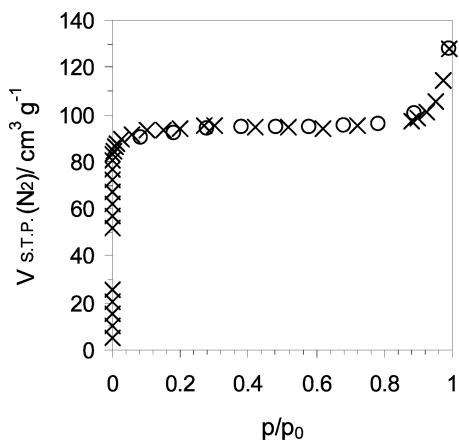


Fig. 4 Nitrogen adsorption (solid symbols) and desorption (open symbols) isotherms of AM-18.

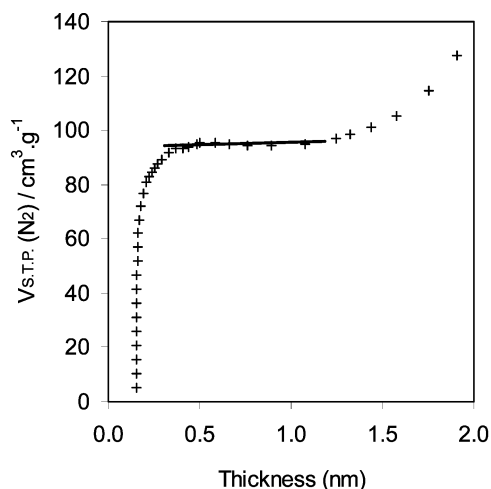


Fig. 5 The t-plot of AM-18 obtained from the N_2 adsorption isotherm.

similar to that derived from the N_2 adsorption data (Fig. 6). AM-18 also adsorbs *m*-xylene and mesitylene, which, unlike benzene, are unable to penetrate in medium pores due to their larger molecular dimensions (7.4 and 8.4 Å, respectively). The adsorption capacities taken at $p/p_0 \approx 0.5$ decreased from 1.14 mmol g^{-1} for *m*-xylene to 0.89 mmol g^{-1} for mesitylene. The above results suggest that the structure of AM-18 possesses

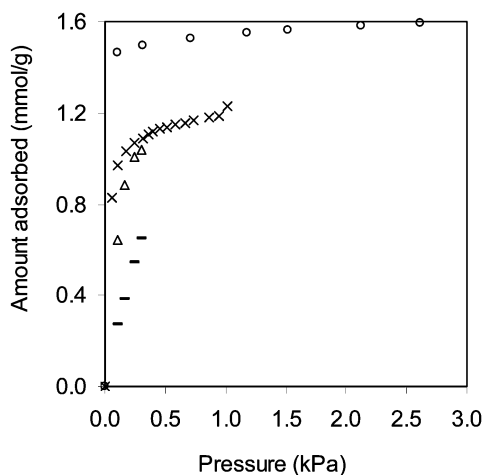


Fig. 6 AM-18 adsorption isotherms for benzene (O), *m*-xylene (x), mesitylene (Δ). ETS-10 adsorption isotherm for mesitylene (-).

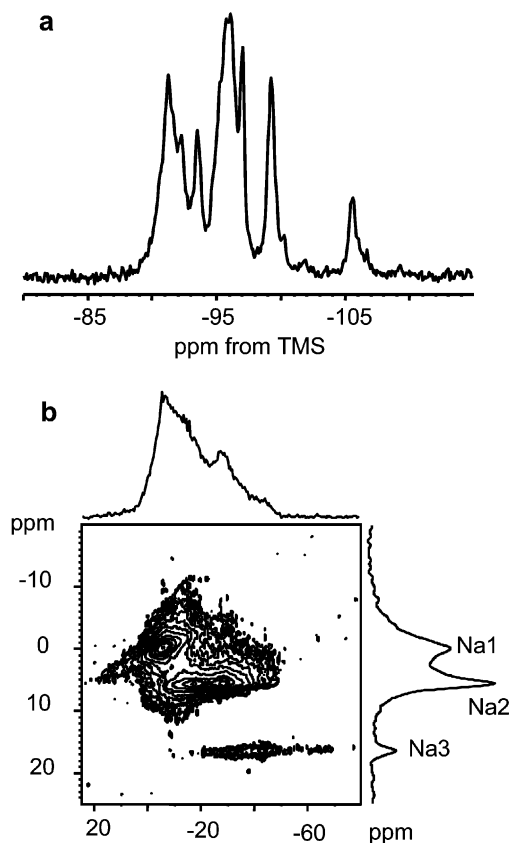


Fig. 7 AM-18 (a) ^{29}Si MAS NMR spectrum (b) ^{23}Na FAM II MQ MAS NMR spectrum.

large accessible pores connected to the surface. Under the same conditions, mesitylene adsorption capacity of ETS-10 is much lower (0.38 mmol g^{-1}) than that observed for AM-18. Hence, AM-18 is one of the largest-pore stoichiometric titanosilicates prepared so far.

The ^{29}Si MAS NMR spectrum of AM-18 displays several resonances in the region -90 to -106 ppm (Fig. 7a). According to Balmer *et al.*,²⁴ a systematic downfield chemical shift is observed when increasing numbers of titanium polyhedra coordinate a given silicon tetrahedron, which is similar to the trend seen for aluminosilicates. Hence, the peak at -105.6 ppm is assigned to Si (4Si, 0Ti) environment, and the resonances in the range -96.3 to -99.0 ppm are ascribed to Si (3Si, 1Ti) while peaks at -91.3 to -93.5 ppm may be due to Si (2Si, 2Ti) sites. The ^{23}Na triple-quantum MAS NMR spectrum of AM-18 has been recorded using a recently introduced modification of MQ MAS spectroscopy known as FAM II MQ MAS (Fig. 7b).²⁵ This technique allows a very efficient conversion of the MQ coherences into single-quantum magnetizations and is particularly well suited for the observation of distorted local Na sites (large quadrupole coupling constants), which is the case of Na3 in AM-18. FAM II MQ MAS shows the presence of three Na sites in AM-18.

Figures 8 and 9 illustrate the infrared and Raman spectra. Both techniques indicate that AM-18 may contain five-coordinated titanium. The Raman spectrum of AM-18 displays a main peak at 806 cm^{-1} (Fig. 8). Raman bands occurring in the range 800 to 900 cm^{-1} in titanosilicate minerals containing exclusively five-coordinated titanium are assigned to the axial Ti–O bond stretch.²⁶ One such material is synthetic layered AM-1 (also known as JDF-L1), which gives a peak at 878 cm^{-1} . In addition, synthetic titanium silicate ETS-4 gives a small Raman peak at 850 cm^{-1} attributed to five-coordinated Ti.^{13,27,28} AM-1 displays a FTIR band at 898 cm^{-1} ascribed to Ti=O stretching vibration, while AM-18 gives a band in the

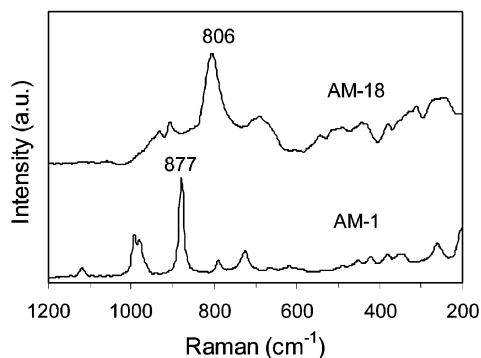


Fig. 8 Raman spectra of AM-18 and AM-1 measured at room temperature.

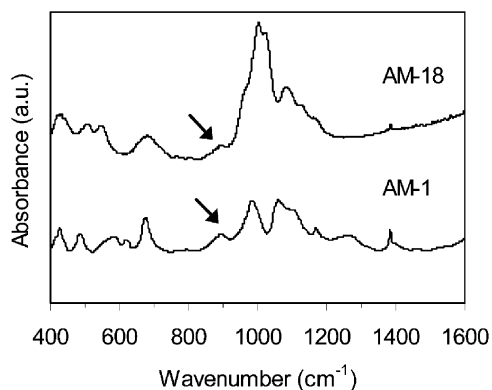


Fig. 9 FTIR spectra of AM-18 and AM-1. The arrows depict the peaks attributed to the Ti=O stretching vibration.

Table 2 Catalytic results (wt%) of isopropanol over AM-18 and ETS-10^a

	AM-18	ETS-10
Conversion	71	29
Acetone selectivity	26	78
Propene selectivity	74	22

^a $T_{\text{reaction}} = 350\text{ }^{\circ}\text{C}$; TOS = 60 min; WHSV = $2\text{ g}_{\text{isopropanol}}\cdot\text{g}_{\text{catal}}^{-1}\cdot\text{h}^{-1}$, Carrier gas—Argon.

same spectral region at 899 cm^{-1} (Fig. 9). ETS-4 displays a FTIR band at 830 cm^{-1} .¹³ After ETS-4 and AM-1, AM-18 is most likely the third known synthetic microporous titanium silicate material containing five-coordinated Ti.

The catalytic performance of AM-18 and microporous titanium silicate ETS-10 was compared for the probe reaction of isopropanol conversion.²⁹ AM-18 is more active than ETS-10 by a factor of two (Table 2). The main products are propene and acetone, resulting from acid-catalysed dehydration and base-catalysed dehydrogenation, respectively. On the basis of acetone selectivity, AM-18 is found to be approximately three times less basic than ETS-10.

Conclusion

In conclusion, a novel large-pore titanium silicate, probably containing five-coordinated titanium, has been synthesised and characterised. Given the relatively high thermal stability and

activity of AM-18 for isopropanol conversion (in excess of 70%) further studies are in progress aimed at exploring the potential of this material in other catalytic processes.

Acknowledgements

We acknowledge, PRAXIS XXI and FCT, FEDER and POCTI (Portugal) for financial support and Cláudia Morais for help in collecting the 2D NMR data.

References

- 1 M. Taramasso and B. Notari, US Patent No. 4410501, 1983.
- 2 T. Blasco, M. A. Camblore, A. Corma and J. Perez-Pariente, *J. Am. Chem. Soc.*, 1993, **115**, 11806.
- 3 G. J. Kim, B. R. Cho and J. H. Kim, *Catal. Lett.*, 1993, **22**, 259.
- 4 T. Maschmeyer, F. Rey, G. Sankar and J. M. Thomas, *Nature*, 1995, **378**, 159.
- 5 P. Taneb, M. Chibwe and T. Pinnavaia, *Nature*, 1994, **368**, 321.
- 6 A. Corma, M. T. Navarro and J. Perez-Pariente, *J. Chem. Soc., Chem. Commun.*, 1994, 147.
- 7 J. M. Thomas, *Nature*, 1994, **368**, 289.
- 8 S. M. Kuznicki, US Patent No. 4853202, 1989.
- 9 M. W. Anderson, O. Terasaki, T. Ohsuna, A. Philippou, S. P. Mackay, A. Ferreira, J. Rocha and S. Lidin, *Nature*, 1994, **367**, 347.
- 10 J. Rocha and M. W. Anderson, *Eur. J. Inorg. Chem.*, 2000, 801.
- 11 M. W. Anderson, O. Terasaki, T. Ohsuna, P. J. O'Malley, A. Philippou, S. P. Mackay, A. Ferreira, J. Rocha and S. Lidin, *Philos. Mag. B*, 1995, **71**, 813.
- 12 M. A. Roberts, G. Sankar, J. M. Thomas, R. H. Jones, H. Du, M. Fang, J. Chen, W. Pang and R. Xu, *Nature*, 1996, **381**, 401.
- 13 S. Nair, H.-K. Jeong, A. Chandrasekaran, C. M. Braunbarth, M. Tsapatsis and S. M. Kuznicki, *Chem. Mater.*, 2001, **13**, 4247.
- 14 P. A. Sandomirskii and N. V. Belov, *Sov. Phys. Crystallogr. (Engl. Transl.)*, 1979, **24**, 686.
- 15 J. Rocha, P. Brandão, Z. Lin, M. W. Anderson, V. Alfredsson and O. Terasaki, *Angew. Chem., Int. Ed. Engl.*, 1997, **36**, 100.
- 16 P. Brandão, A. Philippou, N. Hanif, P. Ribeiro-Claro, A. Ferreira, M. W. Anderson and J. Rocha, *Chem. Mater.*, 2002, **14**, 1053.
- 17 Z. Lin, J. Rocha, P. Ferreira, A. Thursfield, J. R. Agger and M. W. Anderson, *J. Phys. Chem. B*, 1999, **103**, 957.
- 18 J. Rocha, P. Brandão, Z. Lin, A. P. Esculcas, A. Ferreira and M. W. Anderson, *J. Phys. Chem.*, 1996, **100**, 14978.
- 19 J. Rocha, P. Brandão, A. Philippou and M. W. Anderson, *Chem. Commun.*, 1998, 2687.
- 20 J. Rocha, P. Brandão, A. Philippou and M. W. Anderson, *Chem. Commun.*, 1999, 471.
- 21 A. Ferreira, Z. Lin, J. Rocha, C. M. Morais, M. Lopes and C. Fernandez, *Inorg. Chem.*, 2001, **40**, 3330.
- 22 R. Shirley: *The CRYSFIRE System for Automatic Powder Indexing: User's Manual*, 2000, The Lattice Press, 41 Guildford Park Avenue, Guildford, Surrey GU2 7NL, England.
- 23 J. Laugier and B. Bochu: *Programme D'affinement des Paramètres de Maille à Partir d'un Diagramme de Poudre*, Laboratoire des Matériaux et du Génie Physique, École Nationale Supérieure de Physique de Grenoble (INPG), Domaine Universitaire BP 46, 38402 Saint Martin d'Hères.
- 24 M. L. Balmer, B. C. Bunker, L. Wang, C. F. H. Peden and Y. Su, *J. Phys. Chem. B*, 1997, **101**, 9170.
- 25 A. Goldbourt, P. K. Madhu and S. Vega, *Chem. Phys. Lett.*, 2000, **320**, 448.
- 26 Y. Su, M. L. Balmer and B. C. Bunker, *J. Phys. Chem. B*, 2000, **104**, 8160.
- 27 T. Armaroli, G. Busca, F. Milella, F. Bregani, G. P. Toledo, A. Nastro, P. De Luca, G. Bagnasco and M. Turco, *J. Mater. Chem.*, 2000, **10**, 1699.
- 28 V. Valchev, S. Mintova, B. Mihailova and L. Konstantinov, *Mater. Res. Bull.*, 1996, **31**, 163.
- 29 A. Philippou, J. Rocha and M. W. Anderson, *Catal. Lett.*, 1999, **57**, 151.